9A.2 CROSS VALIDATION OF AIRBORNE RADAR, GROUND VALIDATION RADAR D3R AND DISDROMETER OBSERVATIONS DURING GCPEX

Minda Le * and V. Chandrasekar

Colorado State University
1373, campus Delivery
Fort Collins CO 80523-1373, USA

ABSTRACT

The GPM Cold-season Precipitation Experiment (GCPEx) was held in 2012, Canada. Its primary goal is to improve the GPM snowfall retrieval algorithm through collecting and analyzing datasets from both airborne and ground based remote sensing instruments. NASA DC-8 aircraft carries the second-generation Airborne Precipitation Radar (APR-2) as a prototype of an advanced dual-frequency space radar which emulates DPR on board the GPM core satellite. APR-2 participated in GCPEX experiment and made 14 flights to collect valuable data. The dual-frequency, dual-polarization and Doppler radar (D3R) is a fully polarimetric, scanning weather radar system operating at the same frequency as DPR. The D3R is deployed at CARE site during GCPEx experiment. Two-dimensional video disdrometer (2DVD) are also involved in the experiment. There are five of them located at Bob Morton, Steam Show, Sky Dive, CARE and Huronia sites. In this paper, we study snow as well as rain & mixed phase cases using well aligned datasets from APR-2, D3R and 2DVD. Microphysics retrieved using data from different radar systems are cross-validated. Measured dual-frequency ratio profiles available from APR-2 data are characterized. Some of them can be used to perform simple snow classification.

Index Terms — GPM, Airborne radar, D3R radar, 2DVD, microphysics

1. Introduction

The Global Precipitation Measurement (GPM) mission is an international network of satellites that will provide next-generation global observations of rain and snow. Building upon the success of the Tropical Rainfall Measuring Mission, the GPM concept centers on the deployment of a “core” satellite carrying an advanced radar / radiometer system to measure precipitation from space. The dual-frequency precipitation radar (DPR) will be operating at Ku and Ka band. The GPM core observatory is scheduled for launch in early 2014.

The dual-frequency, dual-polarization and Doppler radar (D3R) is a fully polarimetric, scanning weather radar system operating at the same frequency as DPR, covering a maximum range of 30 km. The D3R is part of GPM ground validation activities. It supports GPM pre-launch algorithm development and contributes to post-launch precipitation product validation.

In GPM pre-launch era, NASA Jet Propulsion Lab developed the second-generation Airborne Precipitation Radar (APR-2) as a prototype of an advanced dual-frequency space radar which emulates DPR on board the GPM core satellite. APR-2 was flown on NASA’s DC-8 aircraft and has participated several important field champions including the Wakasa Bay Experiment in 2003, the NASA African Monsoon Multidisciplinary Analysis (NAMMA) experiment in 2006, the Genesis and Rapid Intensification Processes (GRIP) experiment in 2010 and the GPM Cold-season Precipitation Experiment located in Ontario, Canada in 2012. APR-2 radar provides realistic dual frequency observations that help improve modeling of precipitation microphysics. Especially, for GCPEx experiment, The DC-8 carrying

APR-2 made a total of 14 flights over the period of January 11th to February 25th with the focus on snow precipitation.

Both D3R radar and APR-2 radar were deployed in the GCPEx experiment, which provides us a great opportunity to study and cross-validate the microphysics retrieved from different radar systems. Figure 1 shows the conceptual sampling strategy of GCPEx. In this paper, measured dual-frequency ratio (DFRm) profiles obtained from airborne radar are studied. APR-2 radar pointing downward has fine vertical resolution around 30m. The characteristics of the dual-frequency ratio are studied based on different snow models. Microphysics can be inferred from absolute values of dual-frequency ratio and slope etc. To cross validate the snow microphysics retrieved from airborne radar, well aligned observations from D3R radar are applied. D3R radar has fine range resolution and, besides dual-frequency ratio, D3R radar carries horizontal looking dual-polarization information such as Zdr, Kdp and ρhv, all of which are very useful in hydrometeor detection and snow retrieval.

Two-dimensional video disdrometer (2DVD) are deployed in GCPEx experiment. There are five of them located at Bob Morton, Steam Show, Sky Dive, CARE and Huronia site. Data from Bob Morton (SN25) and Steam Show (SN35) are used in this study to perform cross validate of microphysics. 2DVD has two orthogonally placed line-scan cameras and gives two images of the particle as it falls through the measuring area. It can provide direct information on particle size, number concentration and falling velocity, from which estimate of particle density can be achieved.

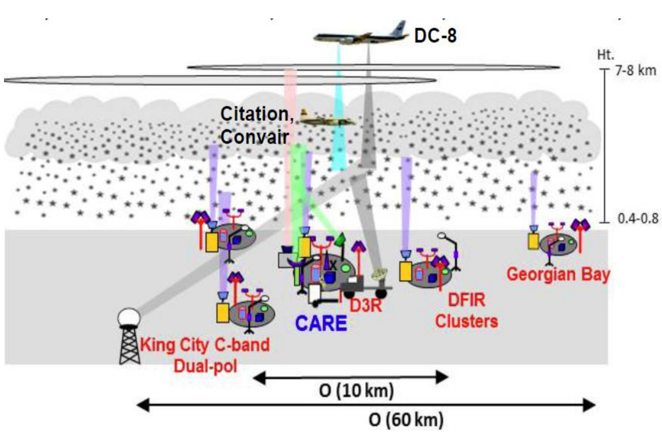

Figure 1, Conceptual sampling strategy of GCPEx (Jackson et al).

D3R radar is located at latitude of 44.232 and longitude of -79.781 degree (CARE site) while APR-2 radar was flying around CARE site, Lake Ontario, Georgian Bay etc. Good RHI scans from D3R were searched with APR-2 scans as close as possible, both physically and temporarily. Effort has been made to find several well matched cases. 2DVD data with the smallest location and time gap were used in the validation. In this paper, three cases on Jan 31, 27 and Feb 24 are chosen for detailed discussion. The case on Jan 31 and Feb 24 are snow only cases. The case on Jan 27 is a rain & mixed phase event.

3, CASE STUDY

3.1 Jan31-2012 (CASE 1)

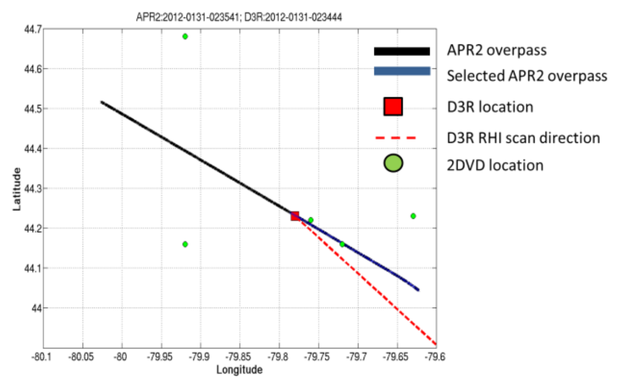

Figure 2. Geolocation of APR-2, D3R and 2DVD in case 1. Black line shows location of APR-2 overpass of 2012-0131-023541. Red dashed line is the RHI scan direction (Azimuthal=150.9 deg) of D3R radar with scan number of 2012-01310023444. Blue part of airborne overpass illustrates the portion that matches with RHI scan. Green circles are locations of 2DVD.

Figure 2 shows the layout of three different instruments: APR-2, D3R and 2DVD, in case 1. Temporal difference between APR-2 and D3R data is only 1-minute apart. The farthest location difference is less than 5km. Figure 3 illustrates the corresponding dataset. Figure 3(a) and (b) are reflectivity at Ku and Ka band. Figure 3(c) to (f) are measured Z, Z_{dr}, ρ_{hv} and ϕ_{dp} from D3R RHI scan. Distance at 0 km in the plots indicates D3R location.

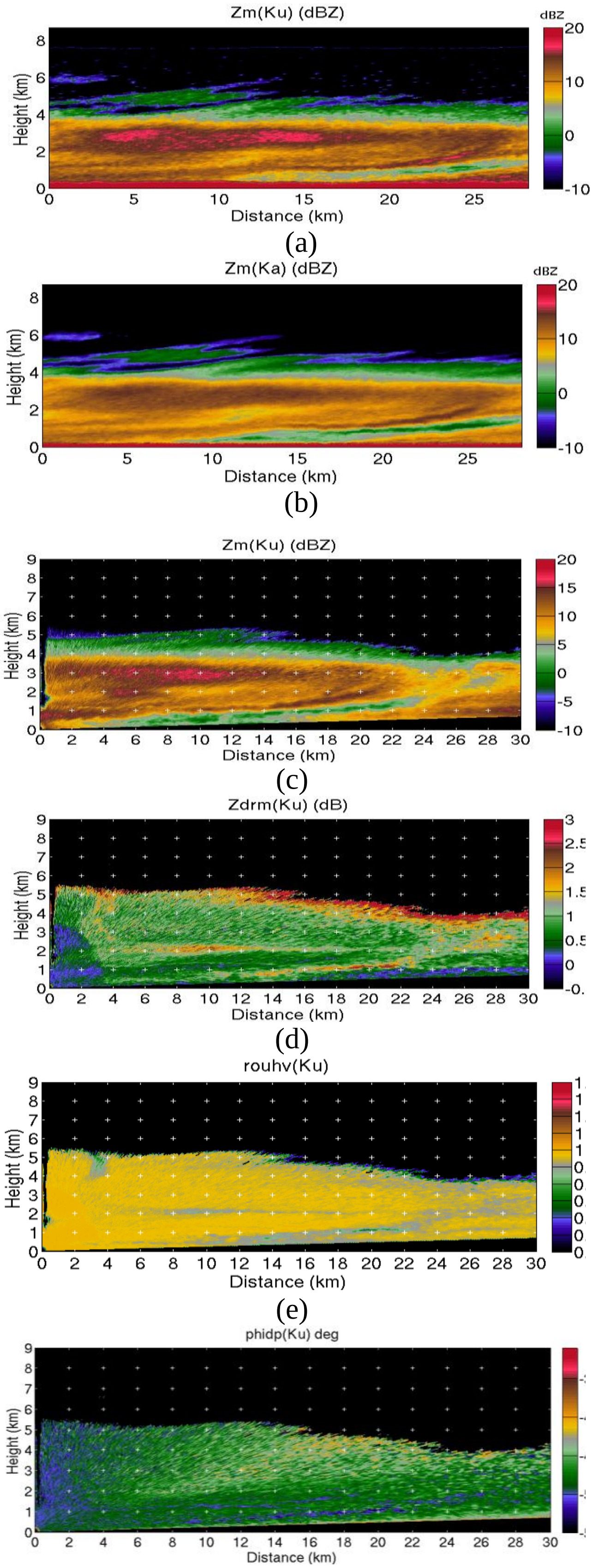

Figure 3 (a) (b) Reflectivity at Ku, Ka band from APR-2. (c) Reflectivity at Ku band from D3R. (d) Differential reflectivity at Ku band from D3R. (e) Copolar cross-correlation coefficient at Ku band from D3R. (f) Differential phase at Ku band from D3R.

From figure 3 (a) and (c), the pattern of reflectivity at Ku from airborne radar and D3R radar match very well. Peak reflectivity reaches 20 dBZ from both radars at around 3km altitude and with range of 5~15 km to radar. Dual-polarized parameters are available from D3R radar. ρ_{hv} from figure 3(e) equals 1 illustrates that, in general, it is a snow case. Relative large Zdr can be found at top of the storm as shown in figure 3(d). This could be caused by ice crystals with strong orientation preference. With decrease of altitude, Zdr decreases which is an indication that aggregation might happen. 2DVD (SN25) took images of the ice particle at Bob Morton site. Figure 4 shows some matched images from the device at different particle sizes. The shape of the images indicates snow. In large shape of aggregates, some air can be found inside the particle. Based on raw drop size distribution as well as falling velocity measured by 2DVD, gamma fitted DSDs and density VS size relation can be estimated (Huang at el. 2010).

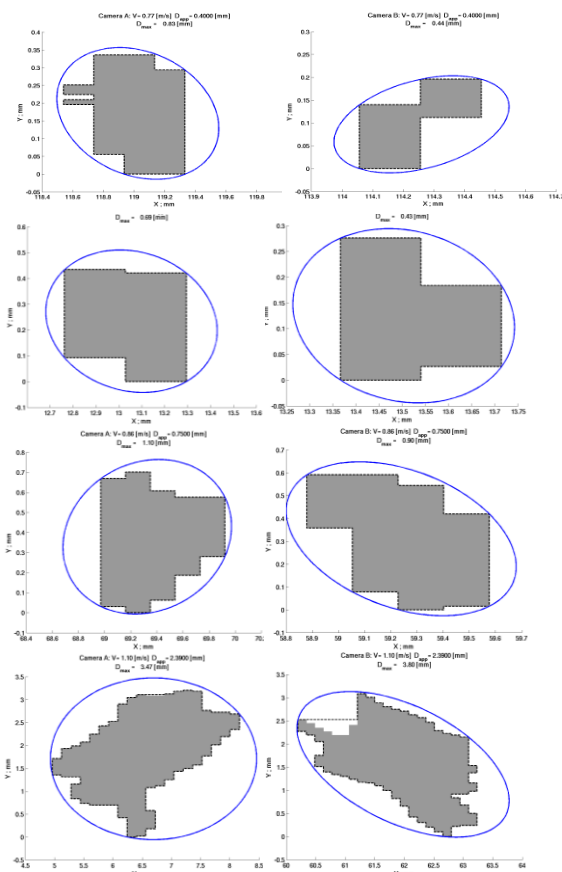

Figure 4 From top to bottom row: randomly chosen 2DVD images from two cameras with drop apparent size of 0.4, 0.43, 0.75 and 2.39 mm.

Figure 5 (a) shows a histogram plot of gamma DSDs at surface (location of SN25) within a 2-hour time window that covers the event time. Density VS size relation can be expressed as a power law relation of ρ=aD^b with coefficient of a and b equals 0.1661 and -0.71747.

APR-2 has good data at both Ku and Ka band as can be seen from figure 3(a) and (b). DSDs are retrieved using dual-frequency ratio retrieval (Meneghini et al. 1997). Since the event is snow, where attenuation can be ignored, forward retrieval is quite accurate and is used in this paper. Density of snow and gamma parameter of μ that constraints the retrieval are taken from 2DVD measurement and estimates. Bulk averaged density equals 0.12 g/cm^3 and μ=0.98 is used in retrieval. Figure 5 (b) illustrates the histogram of retrieved Do and Nw (in log) at surface. Comparing figure 5(a) and (b), both Do and Nw (in log) are within same range of values and they match pretty well. Figure 6 shows the retrieved DSDs for the whole overpass.

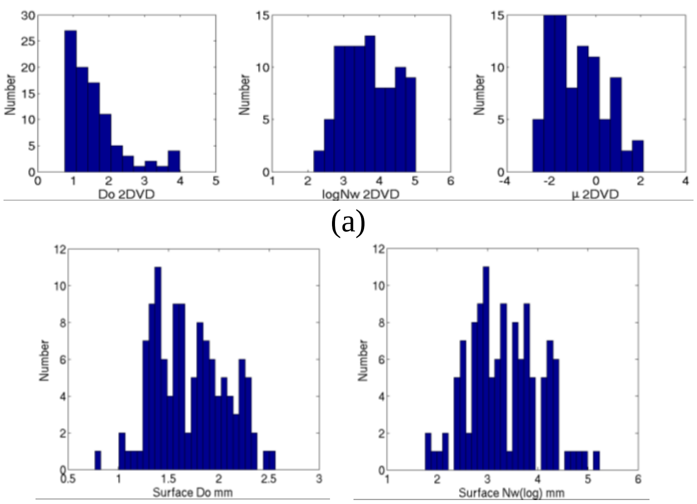

Figure 5 (a) Histogram of gamma DSDs from 2DVD at location of SN25, within 2-hour around event time. (b) Retrieved DSD from airborne radar.

3.2 Feb24-2012 (CASE 2)

Similar to case 1, figure 7 shows the layout of APR-2, D3R and 2DVD in case 2. Temporal difference between APR-2 and D3R data is around 4 minutes apart. The RHI scan line is perfectly aligned with flight direction. Figure 8 illustrates the corresponding dataset which is similar to figure 3.

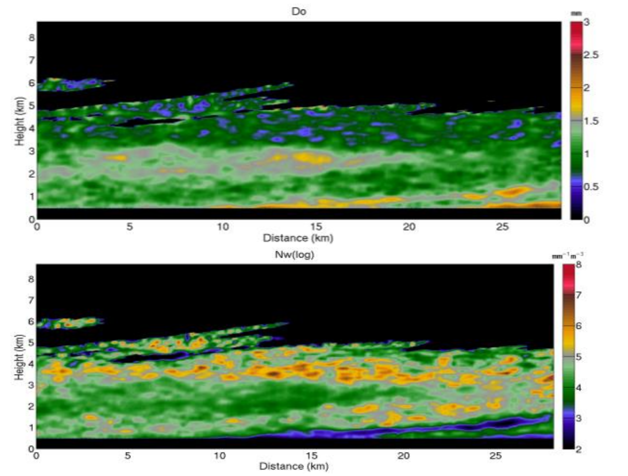

Figure 6 Retrieved Do and Nw (in log) from APR-2 overpass in case 1 using 2DVD estimated microphysics.

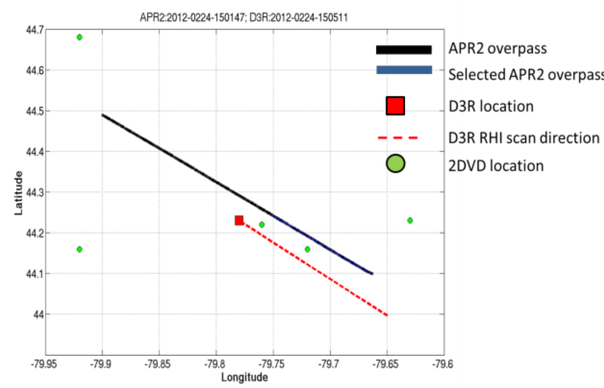

Figure 7 Geolocation of APR-2, D3R and 2DVD in case 2. Black line shows location of APR-2 overpass of 2012-0224-150147;. Red dashed line is the RHI scan direction (Azimuthal=150.9 deg) of D3R radar with scan number of 2012-0224-150511. Blue part of airborne overpass illustrates the portion that matches with RHI scan. Green circles are locations of 2DVD.

D3R radar has good Ka band RHI scan in case 2, and the plot is shown in figure 8 (d). Comparing figure 8(a), (c) and (b) (d), reflectivity field shows great match. At Ku band, peak reflectivity is around 25dBZ from both airborne and D3R radar data which indicates that snow is heavier in case 2 than case 1. Again, dual-polarization parameters from D3R radar shows strong evidence that it is a snow case. 2DVD (SN35) data is used in case 2 analysis. Similar approach that has been described in case 1 was adopted. Figure 9 (a) is

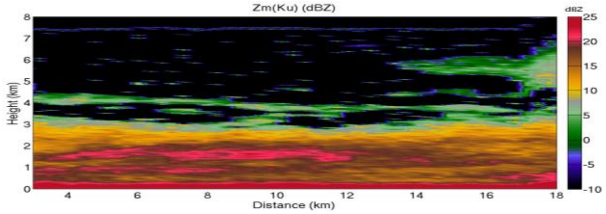

(a)

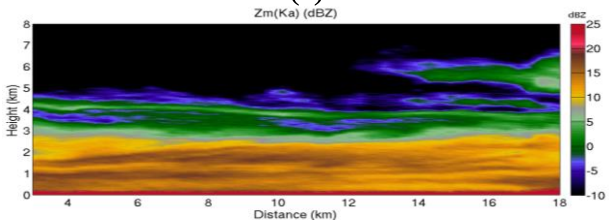

(b)

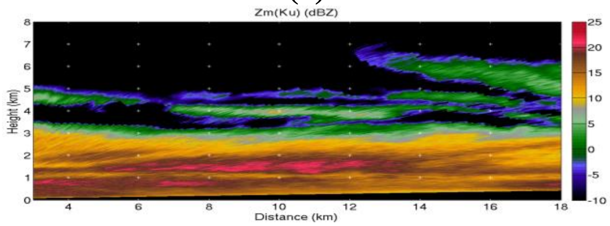

(c)

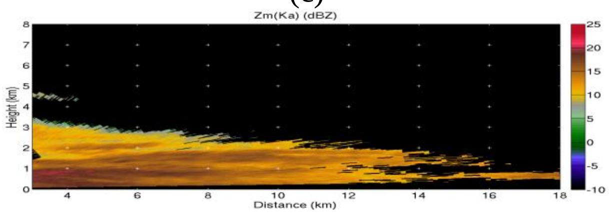

(d)

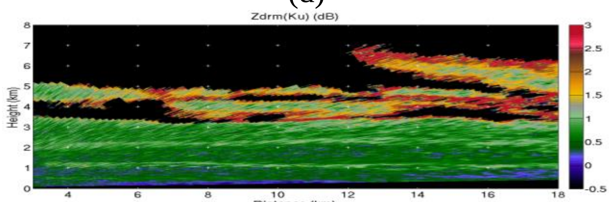

(e)

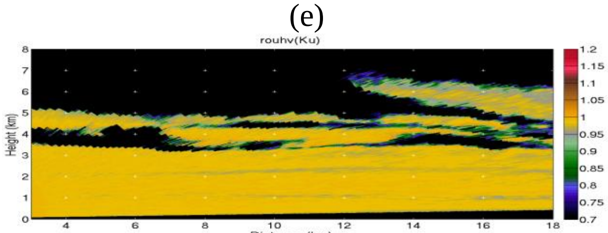

(f)

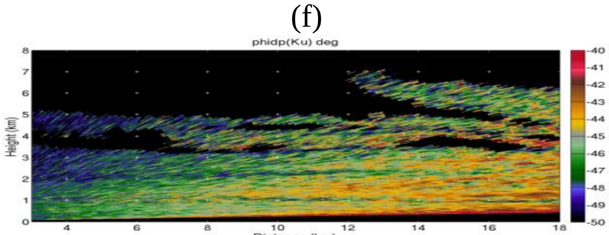

(g)

Figure 8 (a) (b) Reflectivity at Ku, Ka band from APR-2. (c) – (g) Reflectivity at Ku Ka band, Differential reflectivity at Ku, Copolar cross-correlation coefficient at Ku, and Differential phase at Ku band from D3R.

similar to figure 5, showing histogram of gamma DSDs estimated from 2DVD data 1-hour around the event time. The coefficient of density VS size relation, a and b equals 0.2688 and -0.93345 respectively. The bulk averaged density equals 0.26 g/cm^3. Shape factor μ (= -2) was taken from 2DVD at the even time. These microphysics information were used in dual-frequency retrieval and the results are illustrated in figure 9(b). The retrievals from airborne data shows good match with 2DVD surface microphysics.

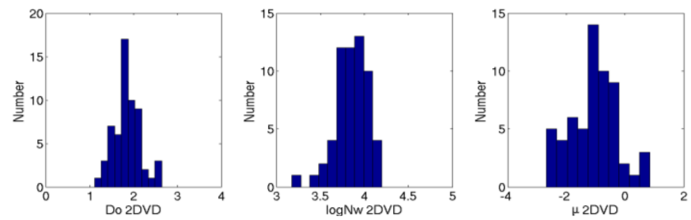

(a)

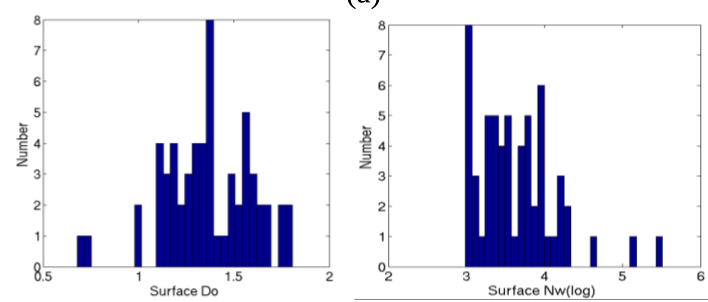

(b)

Figure 9 (a) Histogram of gamma DSDs from 2DVD at location of SN35, within 2-hour around event time. (b) Retrieved DSD from airborne radar.

Retrievals from D3R data using dual-frequency ratio approach are performed. Figure 10 (a) and (b) shows Do retrieved from both APR-2 data and D3R data. Figure 10 (c) and (d) are Nw (in log) from two radar systems. Comparing figure 10 (a) and (b), Do values and pattern from both retrievals matches pretty good. At altitude between 1~2km, and range from 6~15 km from D3R radar, relative large Do (2~2.5 mm) are retrieved from both radars. Correspondingly, large reflectivity values are found at these areas. Zdr from D3R shows relative small values. All these information indicates that aggregations occur in this area. Some discrepancy can be found from Nw retrieval close to D3R radar, as shown in figure 10 (c) and (d). This might due to different forward retrieval direction for different radar, and time difference might also cause the difference. In general, the Do retrievals are comparable.

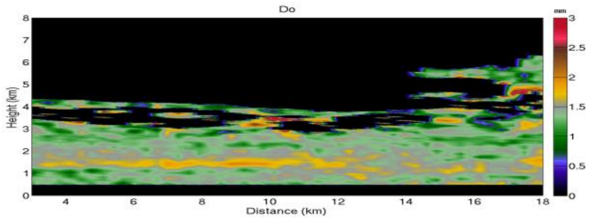

(a)

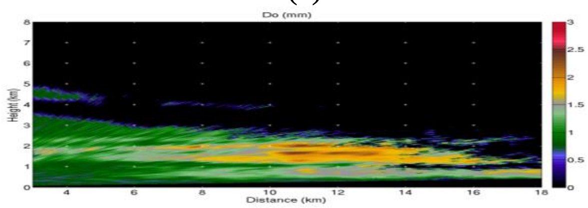

(b)

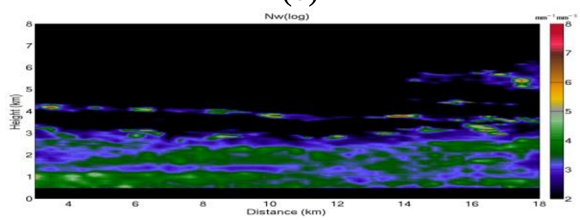

(c)

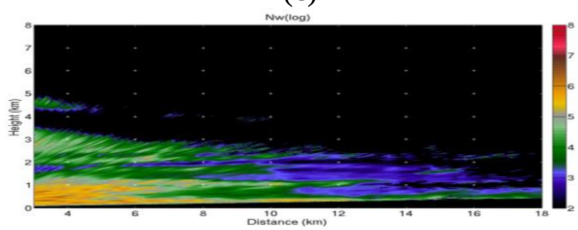

(d)

Figure 10 (a),(b) Do retrieval from APR-2 and D3R data as shown in figure 8. (c) and (d) Nw (in log) retrieval from the same event.

3.3 Jan27-2012 (CASE 3)

The above two cases are snow only cases, and case 3 discussed in this section is a rain & mixed case. Figure 11 illustrates geolocation information of case 3. Temporal difference between APR-2 and D3R data is around 5 minutes apart. The largest gap in geolocation is about 10 km. Figure 12 shows the datasets.

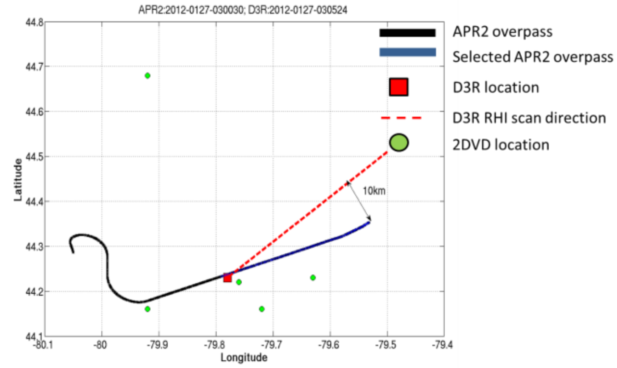

Figure 11 Geolocation of APR-2, D3R and 2DVD in case 3. Black line shows location of APR-2 overpass of 2012-0127-030030;. Red dashed line is the RHI scan direction (Azimuthal=44.97 deg) of D3R radar with scan number of 2012-0127-030524. Blue part of airborne overpass illustrates the portion that matches with RHI scan. Green circles are locations of 2DVD.

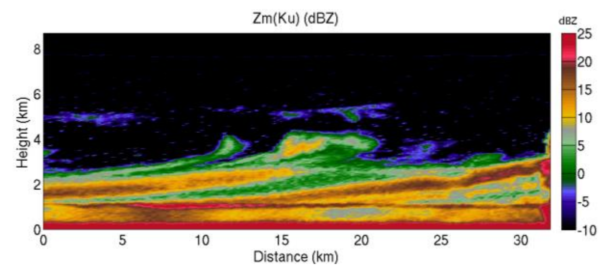

(a)

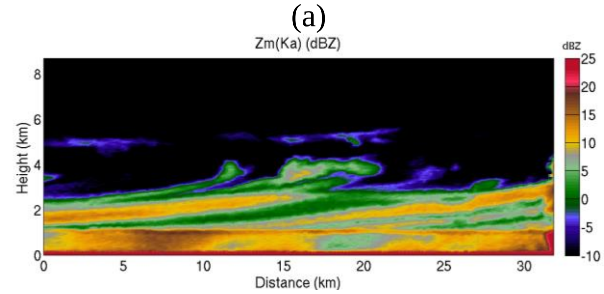

(b)

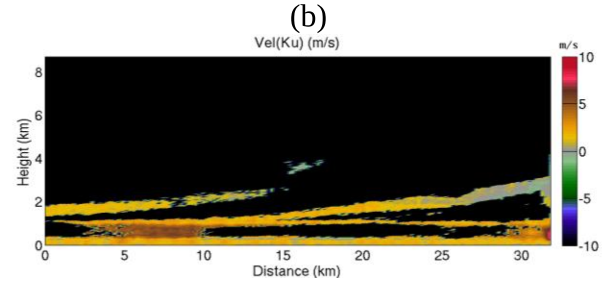

(c)

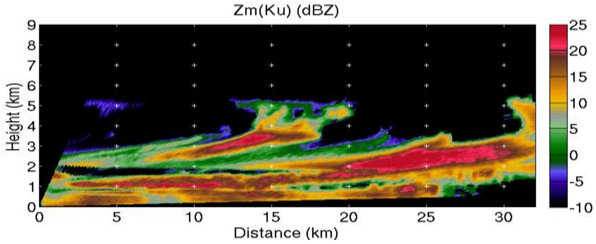

(d)

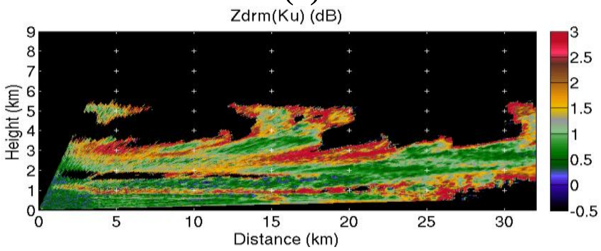

(e)

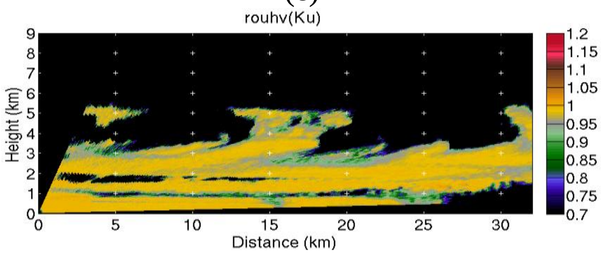

(f)

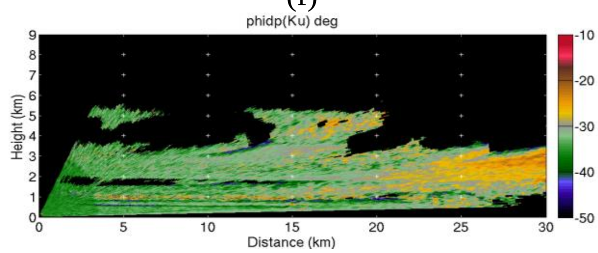

(g)

Figure 12 (a)-(c) reflectivity at Ku, Ka band and Doppler velocity at Ku from APR-2. (d)-(g) reflectivity at Ku, differential reflectivity at Ku, Copolar cross-correlation coefficient at Ku, and Differential phase at Ku band from D3R.

In case 3, bright band can be observed at altitude around 1.2 km from both airborne and D3R data as shown in figure 12. Doppler velocity from APR-2 (figure 12 (c)) also shows a sudden increase at around 1.5 km and then relative constant values below that. From D3R dual-polarization data, phv decreases to around 0.9 at the same height and Zdr shows relative large values. All these information indicate that melting layer exists at height around 1~1.3 km. Reflectivity at Ku band from D3R (figure 12 (d)) shows strong echo from 20~30 km away of D3R radar. The values go up to 25 dBZ. Compared information from other dual-polarization parameters. The precipitation is mainly snow with aggregation. Airborne data only see reflectivity values at around 20 dBZ. This might be caused by geolocation difference. 2DVD images (SN35) provides us another approach to confirm that the event is rain. Figure 13 shows a sample image taken from 2DVD during the event time.

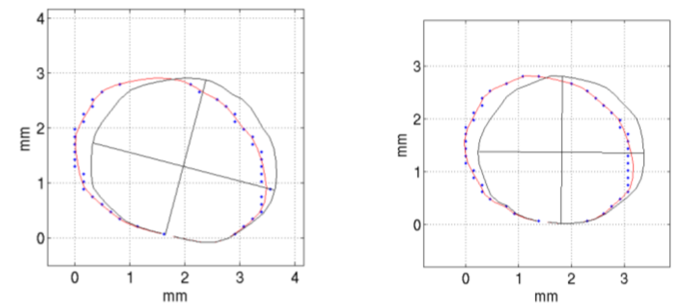

Figure 13 2DVD images of rain on Jan 27. Left plot: front view, the 1402th drop, Deq=3.1, ratio=0.889. Right plot: size view of the matched rain drop.

Figure 14 (a) shows a histogram plot of DSDs estimated from 2DVD data within 4 hour time window. Microphysics from 2DVD were applied in DSD retrievals from airborne data. The retrievals at surface were shown in figure 14 (b). Since only rain microphysics information is available from 2DVD at surface. Some assumptions on snow microphysics are used which could be the reason that retrievals in Nw shows some discrepancy as seen in figure 14.

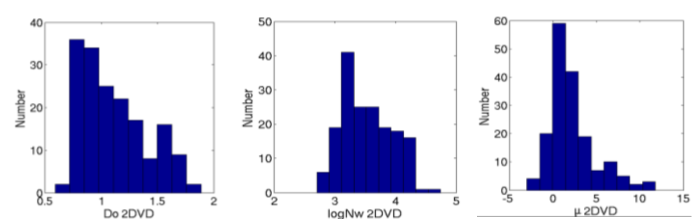

(a)

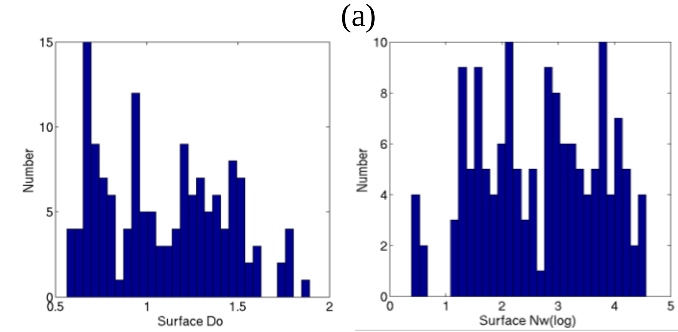

(b)

Figure 14 Histogram of gamma DSDs from 2DVD at location of SN35, within 4-hour around event time. (b) Retrieved DSD from airborne radar.

Figure 15 illustrates a full overpass of retrieved DSDs using algorithm described in Le et al. 2010.

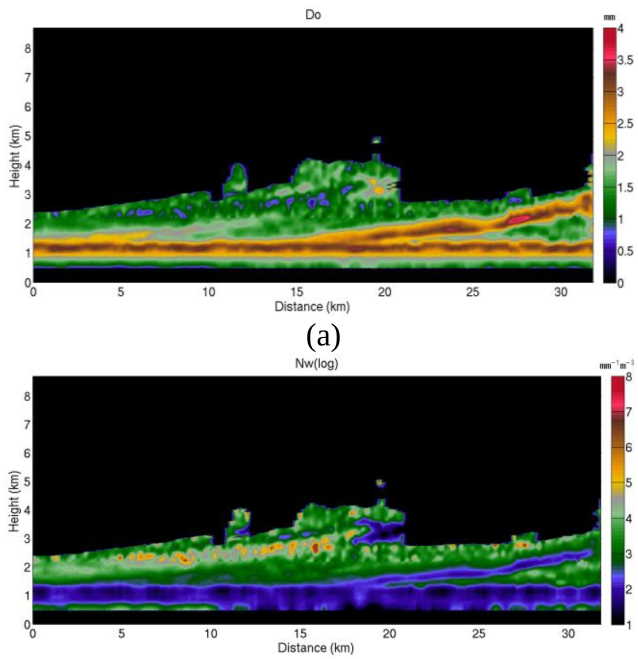

Figure 15 (a) Retrieved Do from APR-2 data (case 3). (b) Retrieved Nw (in log) from the same case.

4, STUDY OF DUAL FREQUENCY RATIO

GCPEx experiment was held in Canada, aiming to study snow microphysics. Airborne radar APR-2 collected good Ku and Ka band vertical profiles during GCPEx. It provides us a great opportunity to study and characterize vertical profiles of measured dual-frequency ratio (DFRm) of snow. The basic concept of measured dual-frequency ratio can be found in Le and Chandrasekar et al. 2012.

In this study, all good vertical profiles of DFRm with snow only are collected and grouped into light, moderate and heavy snow using simple threshold of peak reflectivity value (peak reflectivity @ Ku<15: light snow; >25 heavy snow; moderate snow in between). Different features of DFRm profiles for three groups are extensively studied. These features include mean value of DFRm, slope of DFRm, peak value of DFRm etc. Figure 16 shows the statistics of DFRm mean value for three different groups. From the figure, light snow and heavy snow shows good separation on DFRm mean values. For most of light snow case, DFRm mean values are less than 2 dB. For heavy snow, most of them are above dB. This could be explained through theoretical simulation using different snow models.

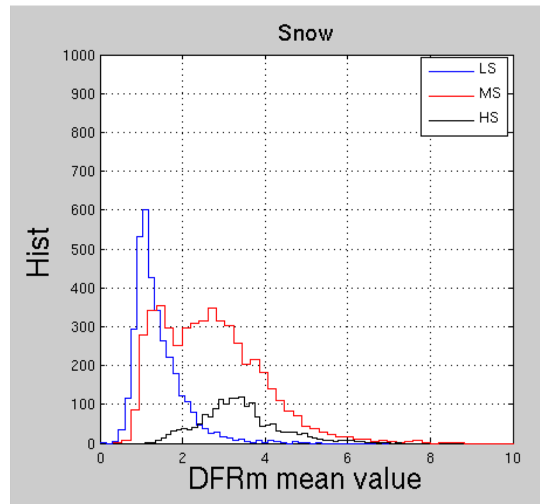

Figure 16 Histogram of DFRm mean slope and mean values for light, moderate and heavy snow using all GCPEx event data (snow part only).

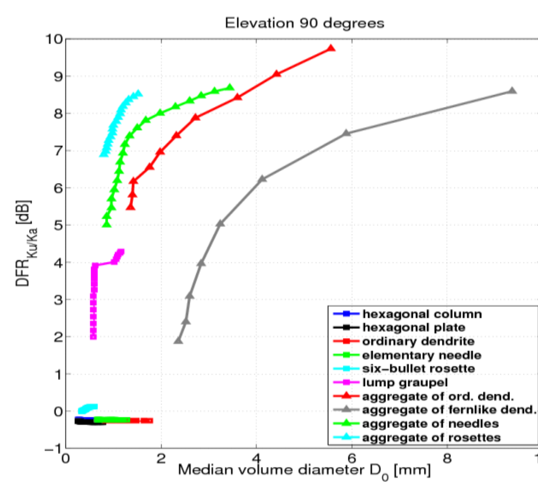

Figure 17 DFR VS Do relation for different snow models. Plots are based on simulation using DDA (Discrete dipole approximation) method. (figure from Tyynelä et al. 2013. Reference: 4th International workshop on space-based snowfall measurement, May 2013, California.)

Figure 17 illustrates a theoretical plot of DFR VS Do using DDA (Discrete dipole approximation) method.

Different curves in the plot can be classified into two classes of snow models. One is ice crystal with different shapes, the other is aggregates of ice crystals. Good separation can be seen easily from figure 17 that dual-frequency ratio values for ice crystals are smaller than 2 dB with most of them close to zero. Under this condition, size of ice crystals are small and Rayleigh scattering dominates the situation. For aggregates, DFR values are larger than 2 dB and could go up to 10 dB for large size of aggregates.

Based on the above analysis, some information of snow type can be inferred from just dual-frequency ratio values. When we look back into figure 16, most of the light snow shows mean DFR values less than 2 dB, indicating that ice crystals dominate the situation. While, for heavy snow, most of the time, DFR values are larger than 2dB, which gives us an idea that aggregation happens. Of course, these analysis are only performed for GCPEx data, different snow depths of snow event in different geolocation might have some effect on the results.

5, SUMMARY

In this study, we perform cross-validation of microphysics retrievals from APR-2, D3R and 2DVD datasets available from GCPEx experiment. Several well aligned cases are found including snow only as well as rain & mixed cases. 2DVD estimated density and DSD information are used in airborne radar data as well as D3R radar data retrieval. Good agreements can be seen. Characterization of measured dual-frequency ratio (DFRm) profile from APR-2 are studied and its mean value provides information on snow classification.

ACKNOWLEDGEMENT

This research is supported by the NASA GPM/PMM program. Authors thank Dr. Jani Tyynelä for providing theoretical simulation results on figure 17. Authors also thank Dr. Gwo-Jong Huang for assistance on processing the disdrometer data.

REFERENCES

Gail Skofronick Jackson, Walter Petersen and Dave Hudak: Let It Snow: GPM Cold-season Precipitation Experiment (GCPEx) Observations to Improve GPM Satellite Methods for Detecting and Measuring Falling Snow.(source:http://atmospheres.gsfc.nasa.gov/science/).

Gwo-Jong Huang, V. N Bringi, Robert Cifelli. David Hudak and W. A. Petersen: A methodology to derive radar reflectivity-liquid equivalent snow rate relations using C-band radar and a 2D video disdrometer. *J. Atmos. Oceanic Technol.*, 27, 637-651.2010.

Meneghini, R., H. Kumagai, J. R. Wang, T. Iguchi, and T. Kozu, 1997: Microphysical retrievals over stratiform rain using measurements from an airborne dual-wavelength radar radiometer. IEEE Trans. Geosci. Remote Sens., vol. 35, no. 3, pp. 487-506.

M. Le ,V. Chandrasekar and S. Lim, Microphysical retrieval from dual-frequency precipitation radar board GPM, Geoscience science and remote sensing symposium, *IGARSS'2010,* IEEE International, Honolulu, USA.

M. Le and V. Chandrasekar, Precipitation Type Classification Method for Dual Frequency Precipitation Radar (DPR) on board the GPM, *IEEE Transactions on Geoscience and Remote Sensing*, Volume 51, issue 3, 2012.